



Jet Propulsion Laboratory
California Institute of Technology

Roman CGI

Observing Scenario 11

Time Series Simulations

(Shaped Pupil Coronagraph
Wide Field of View, Band 4)

John Krist

(Jet Propulsion Laboratory, California Inst. of Technology)

Revised 5 July 2023 (flight DMs, with/without MUFs)

Revised 3 March 2024 (fixed XCENTER,YCENTER header keyword values)

Original 15 February 2022

Acknowledgements

CGI thermal & structural finite element models (FEMs): Josh Kempenaar, Will Krieger Roman & CGI FEM integration, OS11 reaction wheel speeds, spacecraft FEM: NASA Goddard Integrated Modeling Team

CGI pointing jitter model: David Arndt, Nanaz Fathpour, Milan Mandic

OS11 definition: Brian Kern

CGI STOP model execution & analysis: John Steeves, Navtej Saini, Charley Noecker

CGI Code V model: Mike Rogers

CGI LOWFS model: Brandon Dube

CGI mask designs: A.J. Riggs, Dwight Moody

CGI diffraction model & time series generation: John Krist

CGI EMCCD model: Bijan Nemati, Sam Miller, Kevin Ludwick (all U. Alabamba, Huntsville)

Preface

- These simulations are intended for evaluating post-processing algorithms
- Observing Scenario 11 (OS11) is representative of a realistic observing sequence, but does not reflect any particular requirements for total observation time, number of rolls, etc. (there is a limit of about $\pm 13^\circ$ on maximum roll relative to the nominal solar normal orientation)
- OS11 is expected to be the last end-to-end time series
- The thermal+structural modeling results are significantly better than requirements
- The diffraction models intentionally include misalignments, fabrication errors, and uncertainties and do not produce the best possible dark holes, but also may be better than what we really get (they are better than requirements).

Some definitions

- **primary-normalized flux**: image is normalized to the flux incident on the illuminated area of the primary mirror. There are no losses from reflections, filters, QE, etc, but there are losses from masks. In the absence of masks, the total image intensity would be 1.0 over an unlimited extent.
- **normalized intensity**: the per-pixel brightness of the dark hole divided by the peak pixel of the unocculted star. This is sort of a poor man's contrast (because it does not account for field variations in the PSF, especially near the IWA).
- **detector sampling**: the detector pixel size is $0.5 \lambda/D$ @ $\lambda = 500 \text{ nm}$ ($0.303 \lambda/D$ @ 825 nm), which is 21.8 mas

Array dimensions are specified here in IDL ordering (fastest-varying index 1st, slowest last).

CGI SPC-WFOV Band 4

- Shaped Pupil Coronagraph – Wide Field of View (SPC-WFOV)
 - A pupil mask redefines the telescope obscuration pattern to create a tailored diffraction pattern at an intermediate focus
 - An annular focal plane mask (FPM) spanning $r = 5.6 - 20.4 \lambda_c/D$
 - Lyot stop (annular)
- Science field is $r = 6 - 20 \lambda_c/D$
- Band 4 is 11.4% width centered at 825 nm
- SPC-WFOV may optionally be used with the polarizers

$$\lambda_c/D = 72.0 \text{ mas for } \lambda_c = 825 \text{ nm}$$

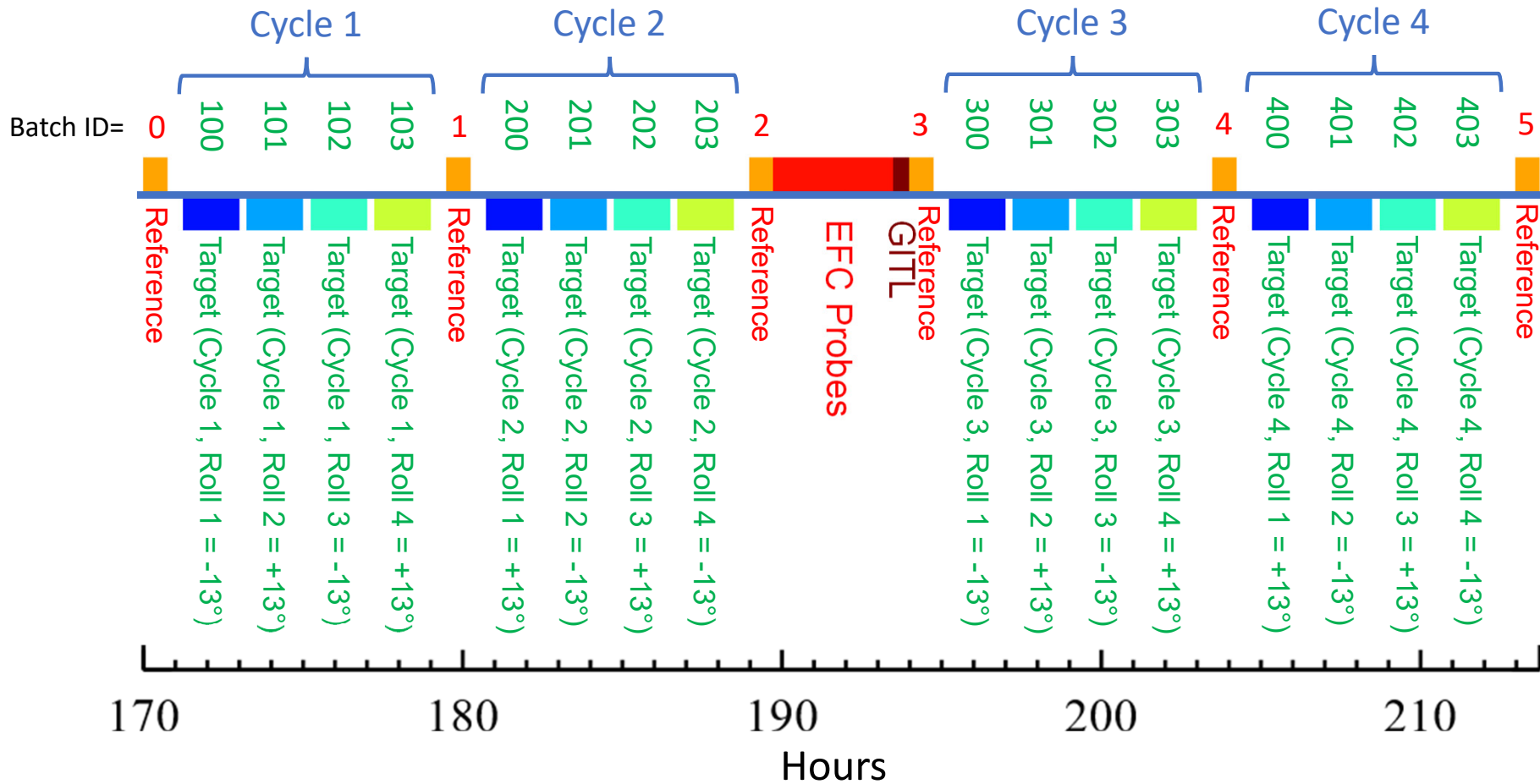
OS 11

- Begin with slew from a WFI High Latitude Survey target to the bright reference star (ζ Pup, $V=2.25$, O4I, $D_{\text{star}}=0.4$ mas), then spend days to settle and restore the dark hole
 - Assume dark hole was previously dug at some earlier time and just needs some tweaking
 - Reference star chosen to keep solar pitch change to $\sim 3.5^\circ$ to avoid large thermal changes
- Observation cycle:
 - $\sim 3/4$ hour of imaging on ζ Pup (1st observation begins at hour 170 in the timeline)
 - slew to the target star (47 UMa, $V=5.04$, G1V, $D_{\text{star}}=0.9$ mas)
 - 100 minutes of imaging 47 UMa at each of 4 rolls, alternating between -13° and $+13^\circ$ for a total of 400 min per cycle
 - slew to ζ Pup
 - $\sim 3/4$ hour of imaging on ζ Pup
- There are 4 cycles, with time between the 2nd and 3rd for one iteration of dark hole maintenance (not reproduced in these simulations)
 - 4.1 hours of total integration on ζ Pup
 - 26.4 hours of total integration on 47 UMa (both roll angles)

OS11 Nomenclature

Reference star images have batch ID's starting with 0 and incrementing by 1 with each visit

Target star images have batch ID's starting with 100 and incrementing by 1 every roll; each cycle of target imaging starts at the next increment of 100



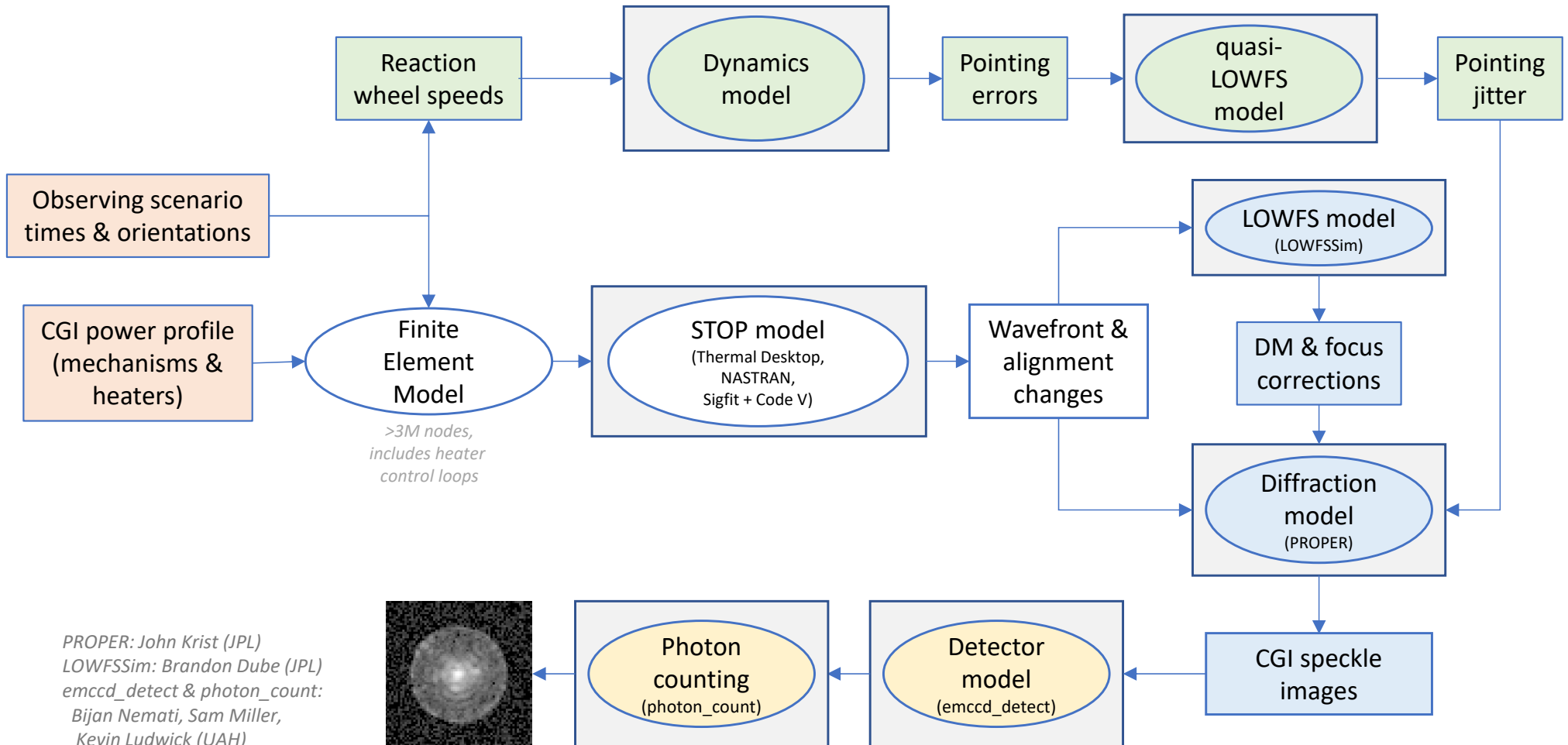
EFC Probes: apply pre-defined DM patterns & record resulting image changes; no images are provided for this span

GITL: Download probe images to ground, use them to derive wavefront error, compute new DM solutions, upload them to CGI

OS11 Modeling Timesteps

- The STOP (finite element & optical ray trace) model was run with 15 min timesteps to derive aberration & alignment changes
 - Misalignment-induced pointing offsets were compensated by repointing the observatory during ray tracing to ensure the star is always perfectly centered on the FPM (this excludes pointing jitter, which is a separate thing)
 - Results were then interpolated to 1 min timesteps
 - Includes thermal effects from solar angles, heaters, CGI mechanism movements (PAMs) & electronics
- The LOWFS model was run to measure aberration changes, which were used to derive DM and focus control compensations in the system model (see later page)
- For each timestep, PROPER produced complex-valued speckle electric fields with $0.1 \lambda_c/D$ sampling for 11 wavelengths at each of 4 polarization states (combinations of $\pm 45^\circ$ in, 0° & 90° out)
- The pointing jitter model, using reaction wheel speeds tailored for OS11, produced RMS X,Y pointing error jitters at 0.25 sec timesteps, interpolated to 1 min timesteps
- At 1st timestep, ΔE -field changes were recorded for a variety of source offsets to create a linear optical model (LOM); At each subsequent timestep, each LOM ΔE -field was added to that timestep's E-field and converted to intensity, creating an ensemble of offset-source images; a weighting function based on the Gaussian jitter & stellar size was applied to these and the resulting images summed to create that timestep's final image (all this was done separately for each wavelength and polarization component)
- The images from the four polarizations were combined
- Appropriate stellar spectra were multiplied by the system throughput curve to weight the monochromatic images, which were then summed to produce broadband images with appropriate flux rates (e-/sec at the detector)
- The images were upsampled via interpolation to 5x-finer-than-CCD pixel sampling, then binned to CCD pixels; these detector-noise-free images are provided as *_noiseless.fits

Simulation Flow (OS 11)



PROPER: John Krist (JPL)
 LOWFSSim: Brandon Dube (JPL)
 emccd_detect & photon_count:
 Bijan Nemat, Sam Miller,
 Kevin Ludwick (UAH)

Errors included in OS11 SPC-WFOV time series optical model

- Static optical errors
 - Measured OTA & TCA (unmounted) optical errors, synthetic CGI optical errors matching measured (but not usable due to artifacts) error maps
 - Stand-in for phase-retrieval-derived optical error map (used for initial phase flattening and in control model); uses computed phase errors at FPM entrance pupil, multiplied by 1.1x to represent phase retrieval errors
 - Polarization aberrations (4 components: orthogonal input terms, orthogonal output terms & cross-terms)
 - Bulk shear of CGI relative to instrument carrier (@ FSM) of 0.14% of pupil diameter
- Z4-Z37 aberrations vs time due to surface deformations & misalignments
- OTA & TCA optics shifts vs time (implemented via shifts of optical error maps)
- Bulk X,Y CGI shear vs time at IC-CGI interface (in addition to initial shear)
- “Known” DM misalignments (included in system & control model)
 - 0.14 mm, -0.14 mm offsets (DM1,2)
 - 0.11°, -0.11° rotations (DM1, 2)
- “Unknown” DM misalignments (addition to known, included in system model but not control)
 - 0.11 mm, -0.11 mm (DM1, 2)
 - 0.1°, -0.1° rotations (DM1, 2)
 - 0.3% mm/actuator spatial scale change
 - DM shifts vs time due to bench deformation, IC-CGI interface tilts
- Measured flight DM characteristics, including dead actuators
- DM bias = 40V, neighbor rule enforced
- 15-bit DAC DM stroke quantization
- CGI DM, pupil mask, & Lyot stop offsets vs time from bench deformations & tilts at IC-CGI interface
- DM surface change due to thermal variations

Note: 1-iteration “refresh” EFC wavefront control in middle of OS11 not included here

Current Modeling Uncertainty Factors (MUFs)

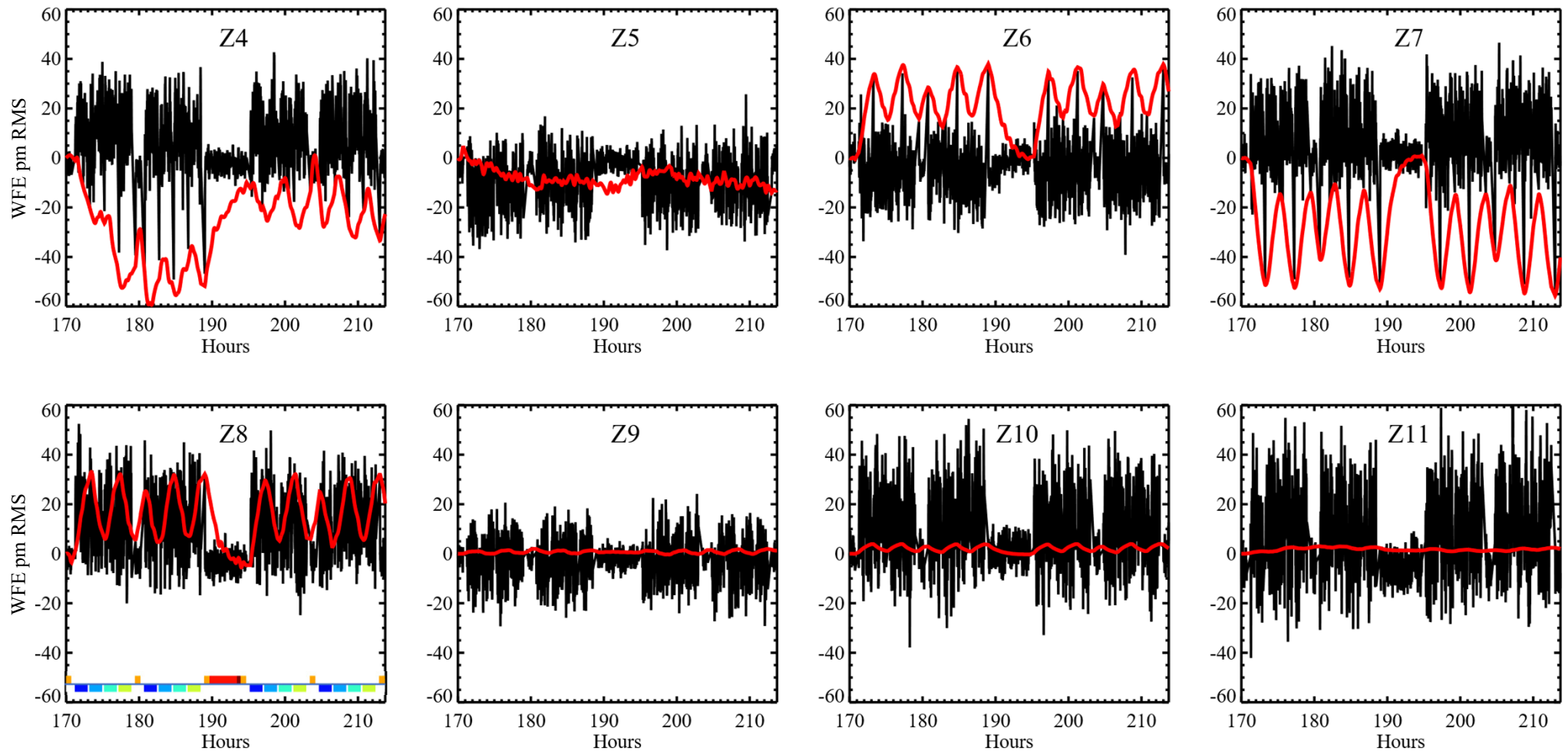
- STOP model (MUF always included)
 - 2x structural deformation MUF
 - increases beam shear, wavefront error drift by 2x
- Dynamic (vibration) model (MUFs always included)
 - Frequency-dependent jitter MUFs
 - 3x (<20 Hz), 4.27x (40-100 Hz), 8x (>100 Hz)
- Diffraction model (only when MUF is indicated)
 - Degraded dark hole contrast (uses the DM patterns from a few EFC iterations prior to the final solution)
 - Higher polarization-dependent aberrations
 - 1.5x higher aberrations
 - 2x higher contrast sensitivity to them
 - Higher pointing error sensitivity
 - 2x in contrast sensitivity (obtained by multiplying jitter by 1.6x)

LOWFS Model

- LOWFS model (LOWFSSim) developed & executed by Brandon Dube (JPL)
 - Diffraction model with STOP-computed Zernikes as input
 - Uses same algorithms as flight for sensing and deriving corrections
 - Includes stellar fluxes & spectral types, detector effects
- LOWFS-measured Zernikes reported every 10 s with 100 s sensing bandwidth
- LOWFS is currently tuned for requirements-level aberration changes, which are much larger than those seen in OS11, so there is significant high-temporal-frequency noise that averages down over the full imaging timescales
- Defocus (Z4) controlled with Focus Correction Mechanism, Z5-Z11 with DM1
- Real LOWFS will be used to measure & control source offsets, but in these simulations those are handled separately when computing jitter

OS11 Zernike Aberrations

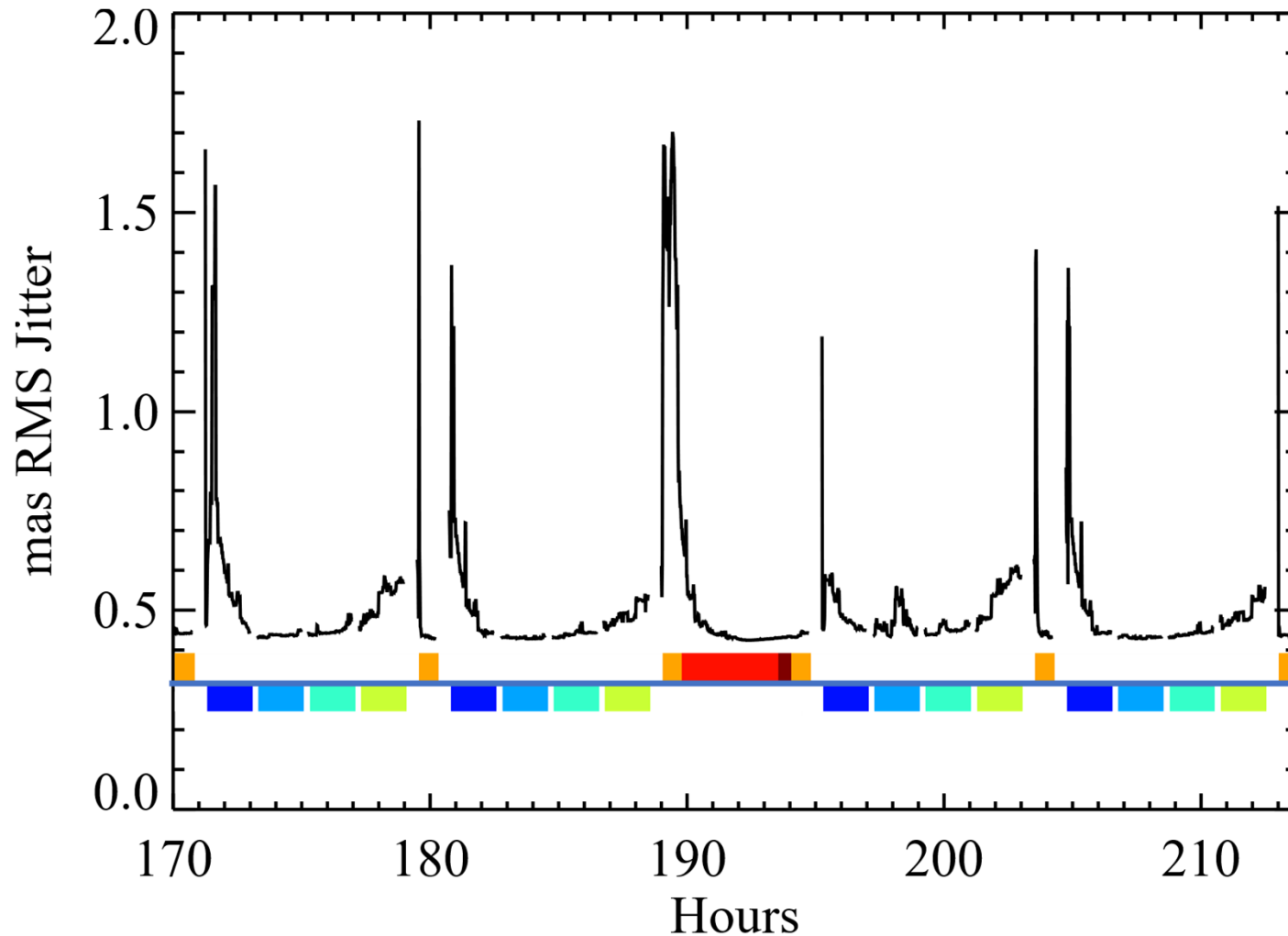
Noll ordering



red = STOP-computed zernikes, black = LOWFS-corrected zernikes (1 m timesteps)

OS11 Post-correction Jitter

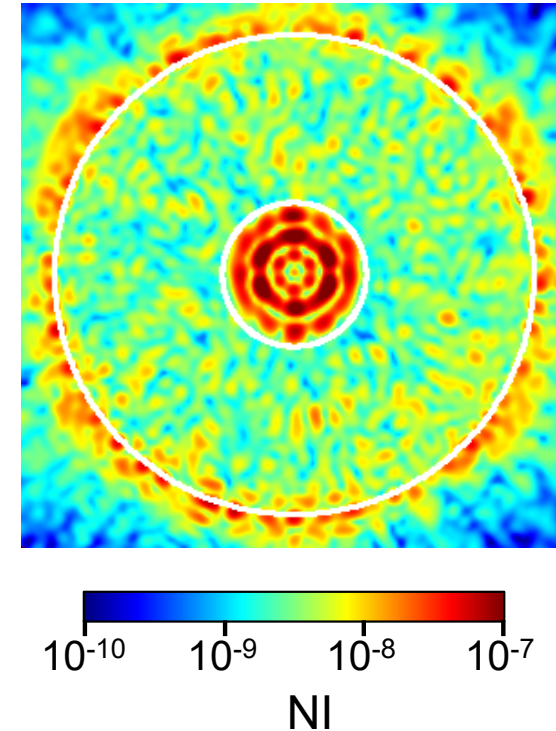
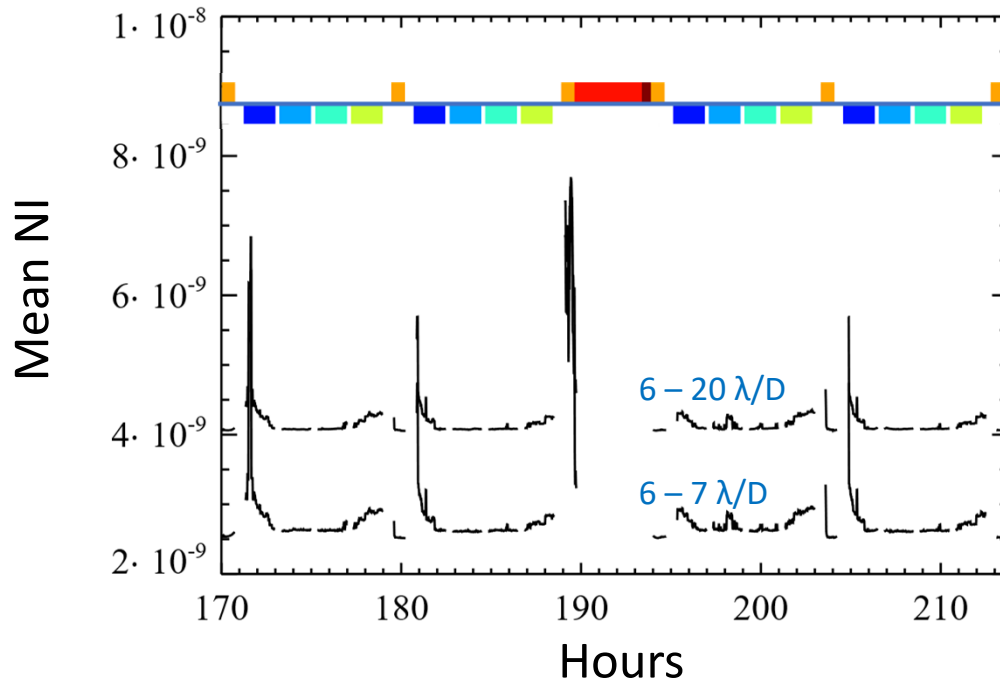
(RSS of X & Y RMS jitters)



The jitter floor here is set by a 0.3 mas RMS (per axis) system noise that is RSSed with the predicted post-steering-mirror jitter.

SPC-WFOV OS11 Dark Hole Mean NI

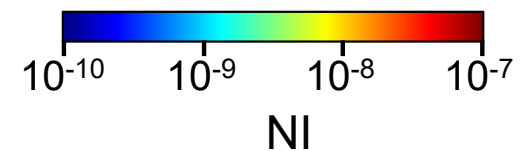
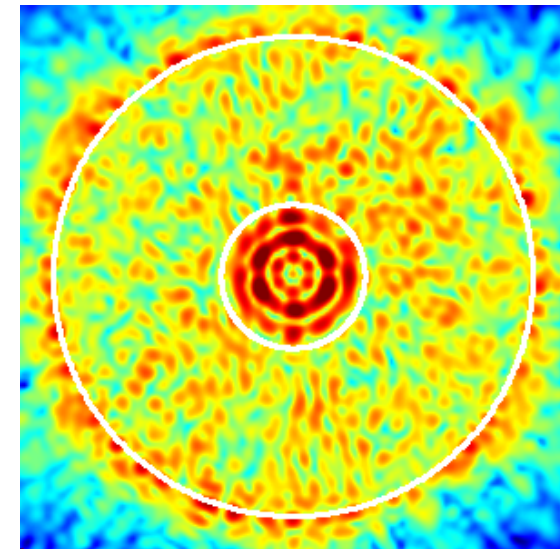
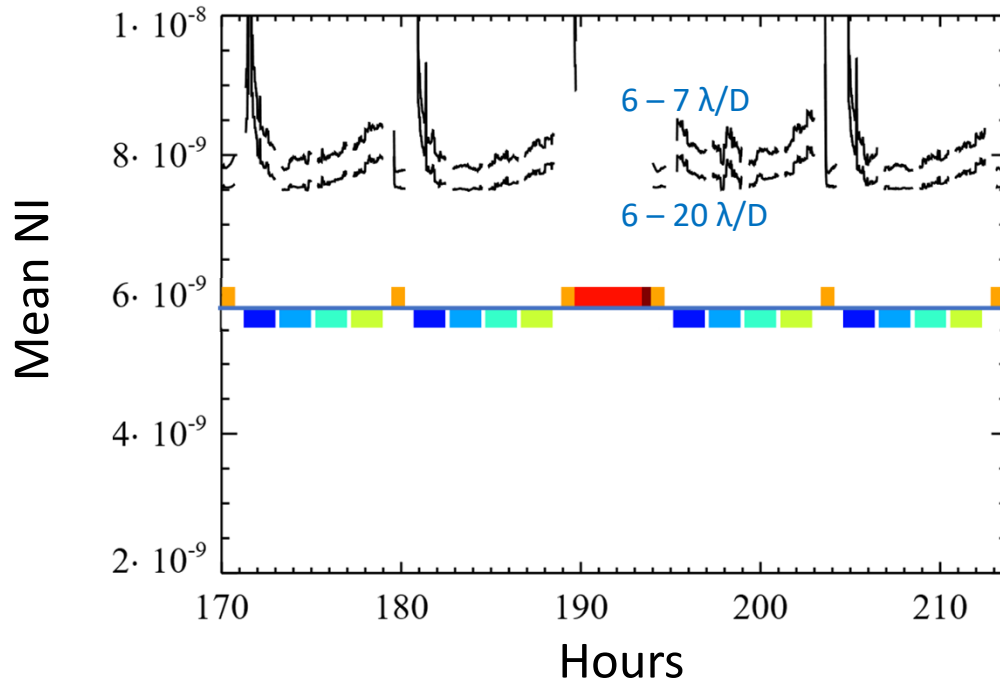
No diffraction MUFs



Mean NI over time:
 2.7×10^{-9} ($3 - 4 \lambda/D$)
 4.3×10^{-9} ($3 - 20 \lambda/D$)

Circles are $r = 6$ & $20 \lambda/D$

SPC-WFOV OS11 Dark Hole Mean NI With diffraction MUFs



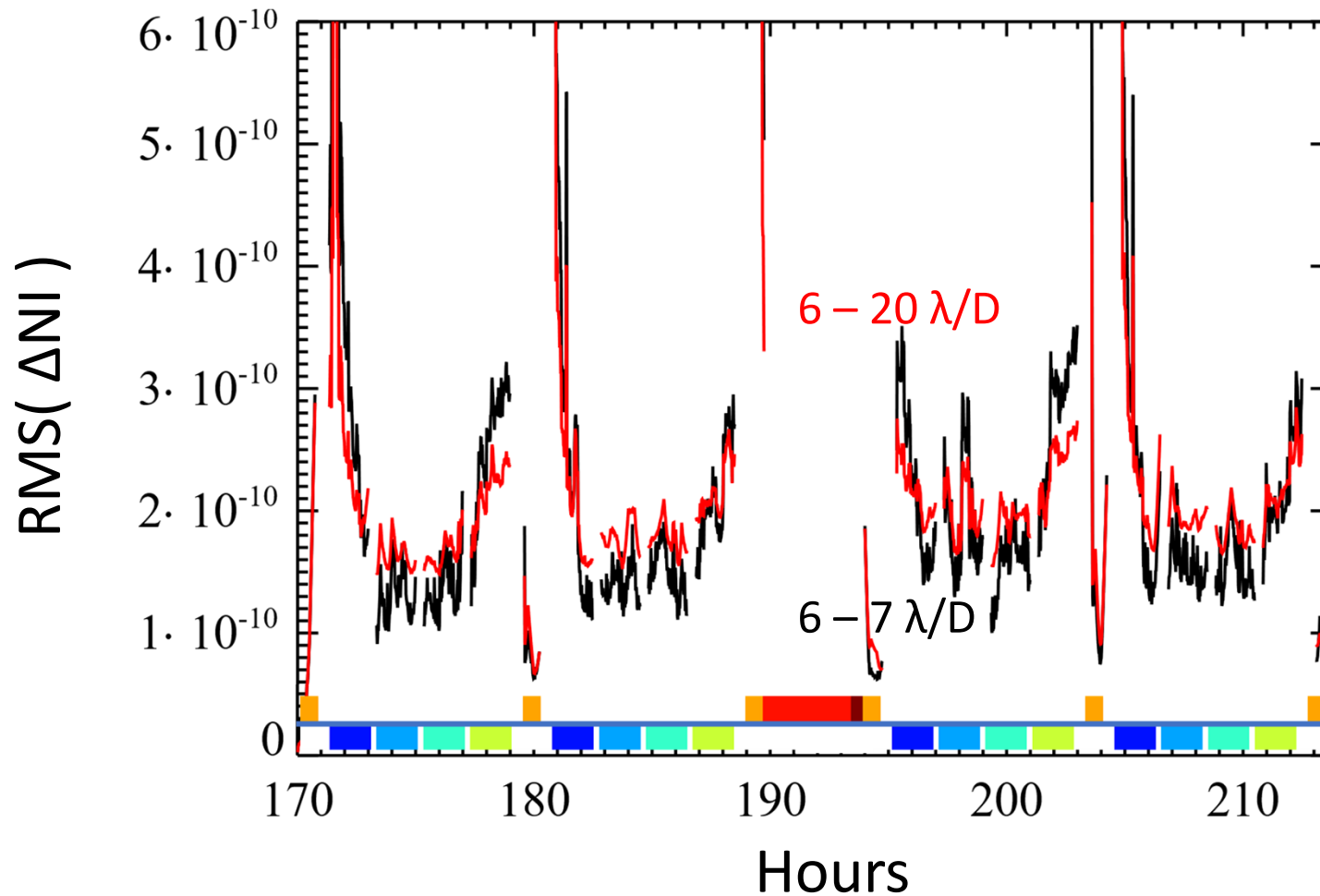
Mean NI over time:

$$8.3 \times 10^{-9} (3 - 4 \lambda/D)$$

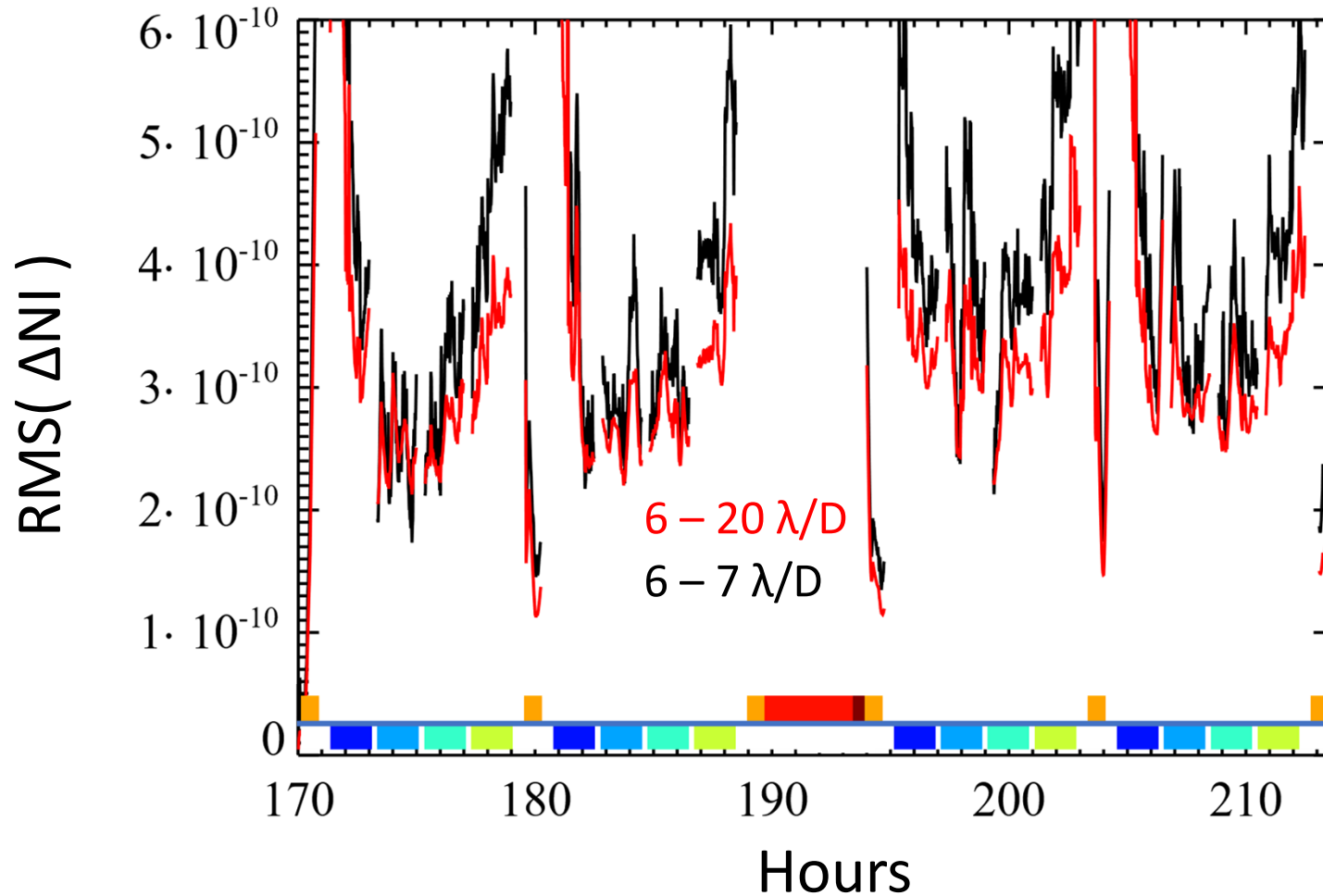
$$7.9 \times 10^{-9} (3 - 20 \lambda/D)$$

Circles are $r = 6$ & $20 \lambda/D$

SPC-WFOV OS11 Dark Hole Difference Relative to 1st Timestep



SPC-WFOV OS11 Dark Hole Difference Relative to 1st Timestep With Diffraction MUFs

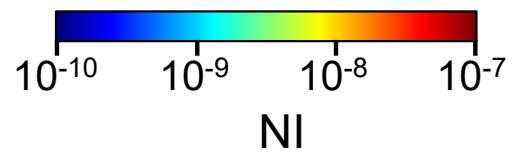
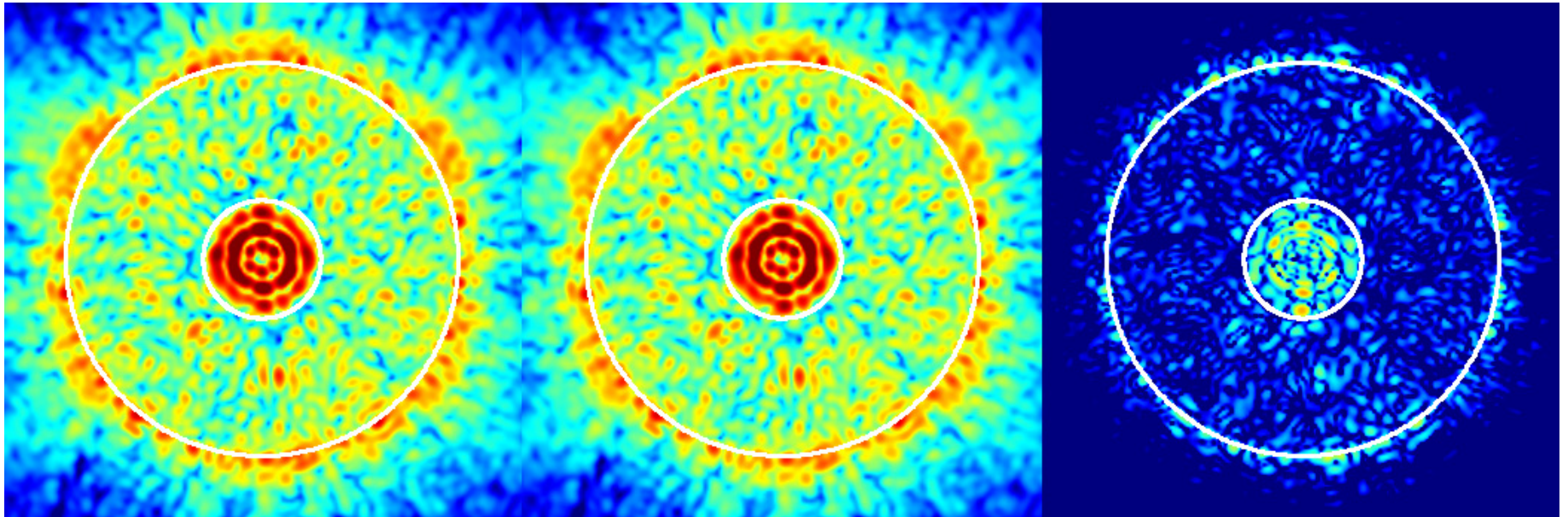


SPC-WFOV OS11 Dark Hole Polarization

0° Polarization

90° Polarization

$|0^\circ - 90^\circ|$



Circles are $r = 6$ & $20 \lambda / D$

SPC-WFOV OS11 Time Series Files

- [spc_wfov_os11_polx_darkhole_noiseless.fits](#), [spc_wfov_os11_poly_darkhole_noiseless.fits](#): OS11 time series speckle field images (no planets) at CCD pixel sampling at 1 minute timesteps. The file dimensions are [nx=181,ny=181,ntimesteps=1830]. This file contains all reference and target star images as generated by the models. Separate files are provided for 0° (polx) and 90° (poly) polarizations. The image values are in electrons/sec (pre-gain) for the given star as detected (includes stellar spectrum & flux and system losses, including QE); these are prior to electron multiplication. The fluxes in each image are half of what they would be without the polarizer (no polarizer losses are included); the images from both polarizations can be added together to produce a no-polarizer image. The input parameters, batch IDs, and other information for each timestep are in the file [spc_wfov_os11_inputs.fits](#) (described on the next page). This file is to be interpolated over time to match chosen camera framerates.
- [spc_wfov_os11_polx_darkhole_noiseless_muf.fits](#), [spc_wfov_os11_poly_darkhole_noiseless_muf.fits](#): As above, but with diffraction MUFs included.
- [spc_wfov_os11_psf_oversampled.fits](#): Simulations of point sources offset from the star by a variety of irregularly-spaced radial offsets and three azimuthal values (0°, 45°, 90°). These images are sampled by $0.1 \lambda_c/D$ ($\lambda_c = 825$ nm; detector sampling is $0.303 \lambda_c/D$). The images are primary-normalized flux. The file dimensions are [nx=555,ny=555,num_radial_offsets=23,num_azimuthal_offsets=4]. The radial and azimuthal offsets are provided in the 1-D FITS files [spc_wfov_os11_psf_radial_offsets.fits](#) [n=23] and [spc_wfov_os11_psf_azimuth_offsets.fits](#) [n=3].
- [spc_wfov_os11_no_fpm_psf.fits](#): Unocculted PSF (star image with no FPM) at CCD sampling; primary-normalized flux units; use to convert dark hole image values to normalized intensity (NI) by (1) multiply PSF by the target or reference star flux, as appropriate, (2) divide the dark hole image by the maximum PSF value.

spc_wfov_os11_inputs.fits

This file is a FITS 2D array, [nterms=81,ntimesteps=1830] providing info for the corresponding image provided in [spc_wfov_os11_darkhole_*.fits](#).

nterm (starting at 0) =

- 0: Time of observation (hours, starting at 170)
- 1: Star ID (1 = target, 2 = reference)
- 2: Batch ID (see OS11 Nomenclature slide)
- 3: Roll; degrees
- 4-45: Input low order aberrations; Noll-ordered Zernikes, Z4-Z45; meters RMS
- 46-53: LOWFS-derived low order corrections (Z4-Z11); meters RMS
- 54-59: Optical surface X shift; [secondary, POMA fold, M3, M4, M5, TT fold]; meters
- 60-65: Optical surface Y shift; meters
- 66-67: CGI X & Y shear at instrument carrier interface (FSM); meters
- 68-69: DM1 X & Y shear; meters
- 70-71: DM2 X & Y shear; meters
- 72-73: DM1 & DM2 temperature; Kelvins
- 74-75: SPAM (SPC pupil mask) X & Y shear; meters (not used for HLC)
- 76-77: LSAM (Lyot stop) X & Y shear; meters
- 78-79: X & Y post-FSM pointing jitter; mas RMS per axis
- 80: Focus correction mechanism offset to compensate Z4; meters

Fluxes

- Flux rates for each star are provided in the header of `spc_wfov_os11_*darkhole*.fits` as the keywords TARGFLUX and REFFLUX
 - rates are appropriate for stellar type and brightness
 - rates are half of what they would be without polarizer (no polarizer transmission losses included)
 - units are total electrons/sec from source *prior to electron multiplication (no gain applied)*
 - includes losses from reflections, filters, QE, but not CGI masks
 - mask losses are included in the image fluxes
- Provided PSFs (`*_psfs*.fits`) are in primary-normalized flux units; to convert to planet e⁻/sec, multiply by planet contrast (e.g., 5e-9) and TARGFLUX

Creating Field Point Sources with CGISim

CGISim is a Python program that generates CGI dark hole and field point source images using the PROPER propagation library and the CGI diffraction model. You can use it to produce field point source images with any offset from the star. It can be downloaded from <https://sourceforge.net/projects/cgisim>. Be sure to read the manual to understand how the images are normalized.

Example code is shown below to generate an off-axis source at $(x,y)=(+570,-100)$ mas.

```
import cgisim_jpl as cgisim
import proper
import roman_phasec_proper_jpl

cgi_mode = 'excam'
cor_type = 'spc-wide'
bandpass = '4'
polaxis = -10 # compute image for mean X+Y polarization

# read in DM patterns provided with Phase C CGI model

file_dir = roman_phasec_proper_jpl.lib_dir + '/examples/'

dm1 = proper.prop_fits_read( file_dir + 'spc_wide_band4_best_contrast_dm1.fits' )
dm2 = proper.prop_fits_read( file_dir + 'spc_wide_band4_best_contrast_dm2.fits' )
params = {'source_x_offset_mas':570.0, 'source_y_offset_mas':-100.0,
          'use_dm1':1, 'dm1_m':dm1, 'use_dm2':1, 'dm2_m':dm2}

psf = cgisim.rcgisim( cgi_mode, cor_type, bandpass, polaxis, params, output_file='psf.fits' )
```

emccd_detect

- **emccd_detect** is a Python package for EMCCD modeling provided by Bijan Nemati, Sam Miller, & Kevin Ludwick from UAH
 - https://github.com/wfirst-cgi/emccd_detect
- The user must specify at least the frame time and EM gain (other parameter have defaults)
 - max gain is 5000
 - Images with gains of <1000 are processed as conventional CCD images (no photon counting), but with high ($100\text{ e}^-/\text{frame}$) read noise
 - shoot for per-pixel flux rates of $\sim 0.1\text{ e}^-/\text{frame}$ (post-amplification) to avoid coincidence losses during photon-counting post-processing
- Output is a “raw” CCD image that must be photon-counted by **PhotonCount**
- CTE not currently included

PhotonCount

- **PhotonCount** is a Python package for EMCCD photon-counting post-processing provided by Bijan Nemati, Sam Miller, & Kevin Ludwick from UAH
 - <https://github.com/wfirst-cgi/PhotonCount>
- The inputs are
 - data cube of raw EMCCD images
 - EM gain
 - photon counting threshold (4x-5x the read noise; I use 500)
- Output image is the mean expected pre-amplified e⁻/frame, corrected for coincidence and threshold losses
- Do not use PhotonCount to process frames taken in analog mode (gain < 1000) – process those like a conventional CCD image (one with high read noise, ~100 e⁻/frame)
- See B. Nemati, “Photon counting and precision photometry for the Roman Space Telescope Coronagraph”, Proc. SPIE, 11443, 114435F (2020)

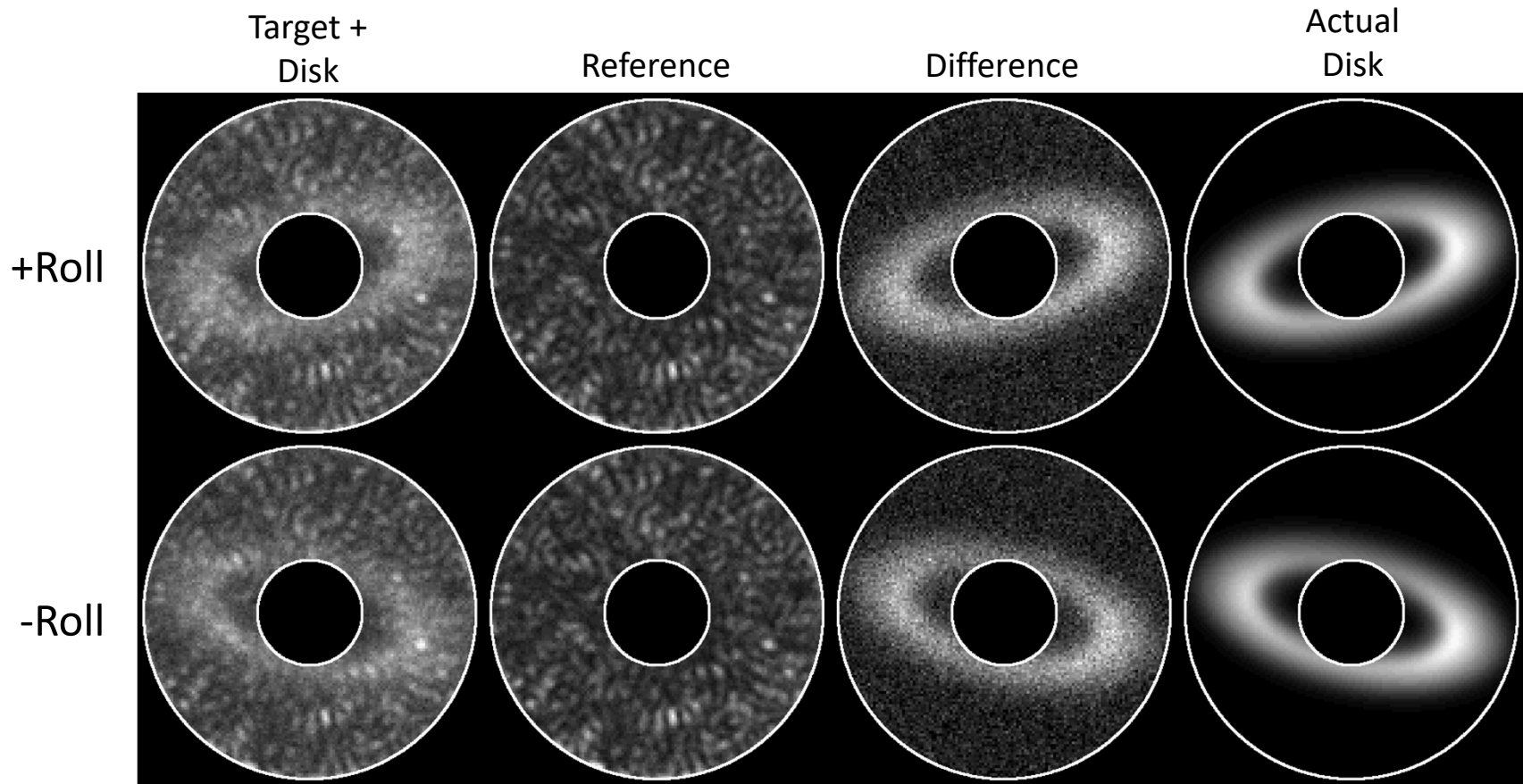
Example Files & Routine

- [spc_wfov_os11_frames_with_disk.fits](#): Temporal resampling of [spc_wfov_os11_*darkhole*.fits](#) (polarizations combined) for 14.0 sec reference star images and 75.0 sec target star images; flux units remain e-/sec (no gain). 0.3 sec separation between frames allocated for readout time.
- [spc_wfov_os11_batch_info.txt](#): Text file listing parameters corresponding to entries, in sequence, in the file [spc_wfov_os11_frames_with_disk.fits](#) for each batch: batch ID, batch start time, star ID, roll, seconds per frame, gain, and number of frames.
- [spc_wfov_os11_example.py](#): Python script illustrating how to process images through `emccd_detect` and `PhotonCount`. Takes as inputs the files listed above, adds EMCCD noise, converts to flux maps, and then does simple RDI to create post-processed planet images. It is assumed that users will use this as a guide and will generate their own image stacks with different gain and exposure times, scenes, etc. Note that cosmic rays are NOT added. Outputs of this script are:
 - [spc_wfov_os11_flux_maps*.fits](#): mean expected flux per batch (photon counting) or mean computed flux per batch (conventional) in e-/sec (no gain), one map per batch
 - [spc_wfov_os11_true_flux_maps*.fits](#): actual mean flux maps from averaging each batch in the noiseless input images file
 - [example_reference_image*.fits](#), [example_target_roll_minus_image*.fits](#), [example_target_roll_plus_image*.fits](#): mean of all reference and target (per roll) images in [spc_wfov_os11_flux_maps*.fits](#)
 - [example_rdi_roll_minus_image*.fits](#), [example_rdi_roll_plus_image*.fits](#): simple RDI results for each roll
- Versions of the FITS image files above are also provided including diffraction MUFs

Results from `spc_wfov_os11_example.py` No diffraction MUFs

All photon-counted frames for each star/roll summed with no rejection

Disk peak-pixel flux equal to a 10^{-8} contrast speckle



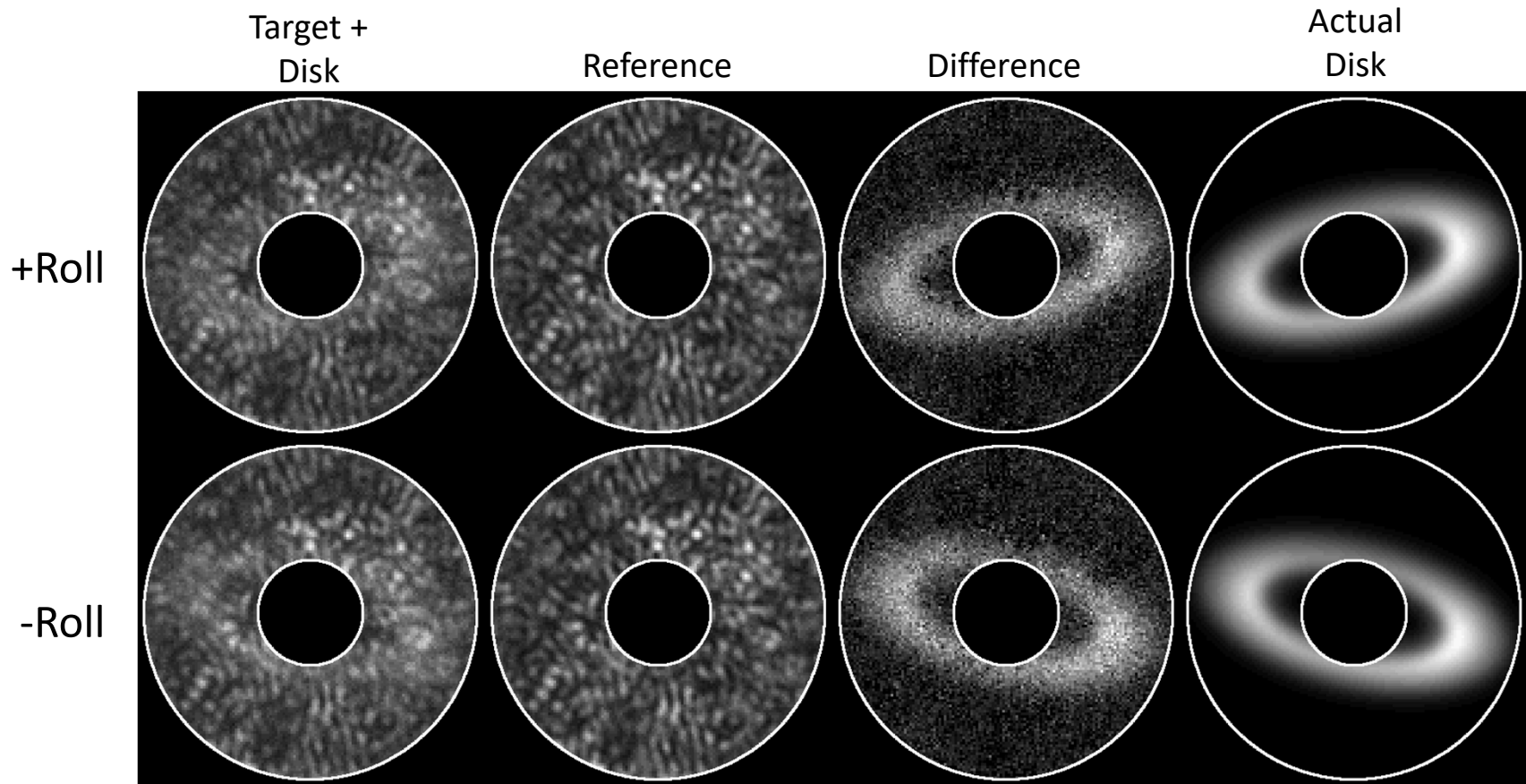
Shown over $r = 6 - 19 \lambda/D$

For simplicity, disk model was convolved with no-FPM PSF

Results from `spc_wfov_os11_example.py` With diffraction MUFs

All photon-counted frames for each star/roll summed with no rejection

Disk peak-pixel flux equal to a 10^{-8} contrast speckle



Shown over $r = 6 - 19 \lambda/D$

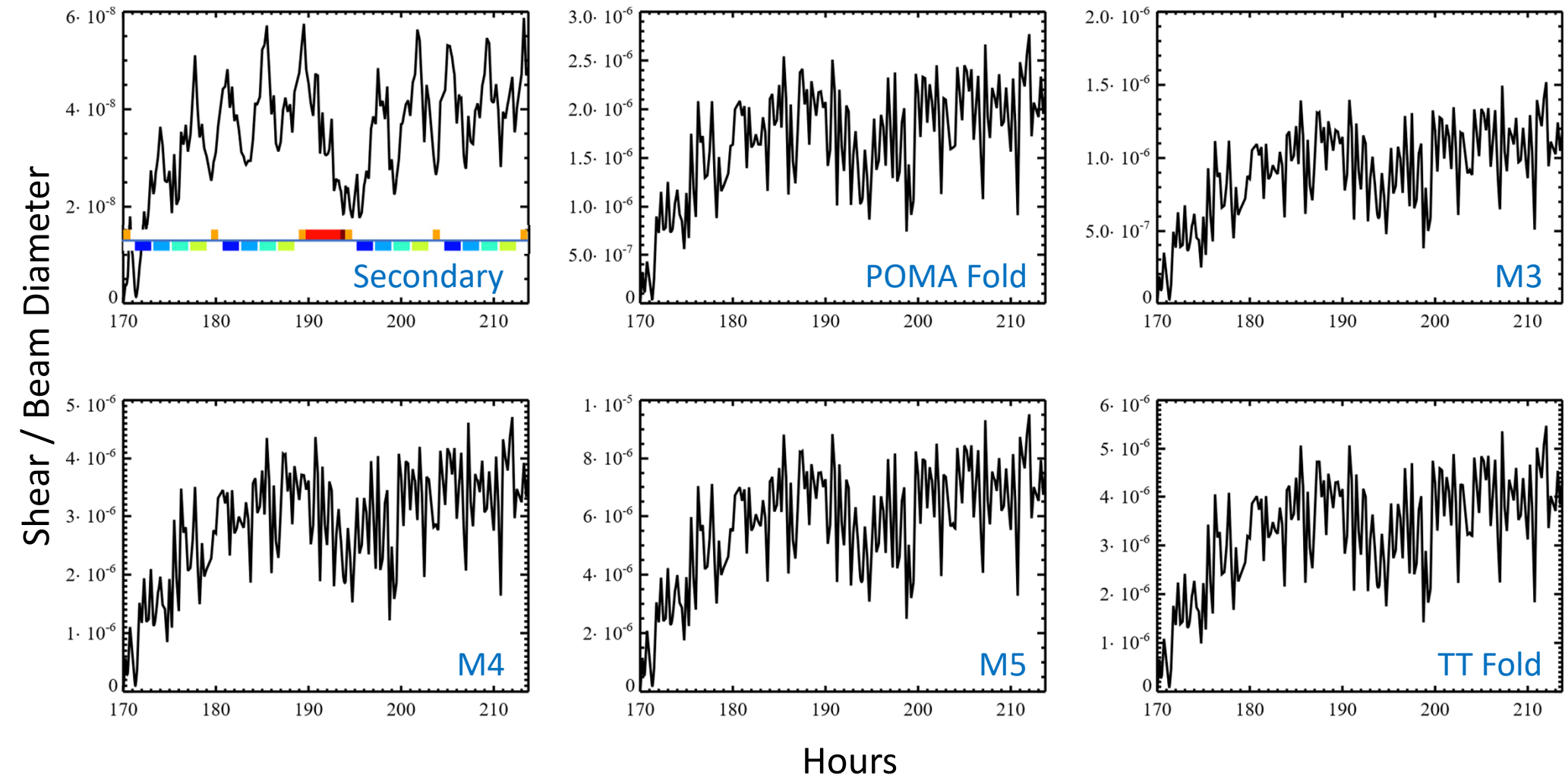
For simplicity, disk model was convolved with no-FPM PSF

Conclusions

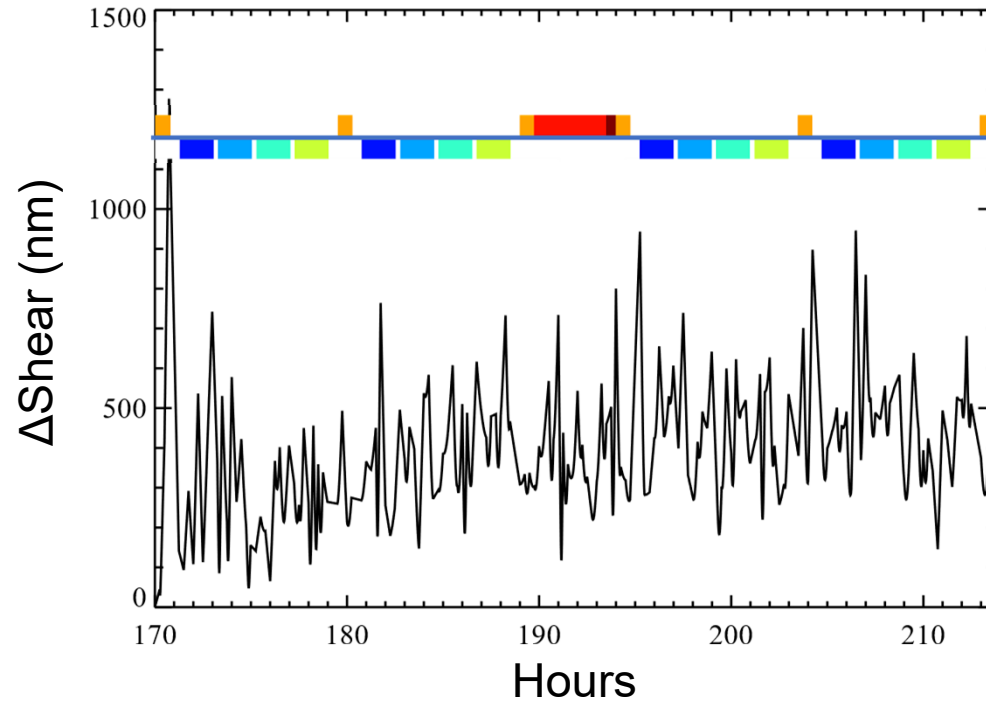
- OS11 results are much better than requirements
- The SPC-WFOV is very tolerant of low-order aberrations (polarization, pointing errors, thermal drifts) due to the nature of the shaped pupil and the large inner working angle
- The SPC-WFOV speckle variations over time as shown here are due mostly to correction of low-order errors by LOWFS with a high-order DM
 - errors largely average out
 - LOWFS tuned for worse aberration drifts than in OS 11
- Detector noise may be a significant limiting factor

Additional STOP Results

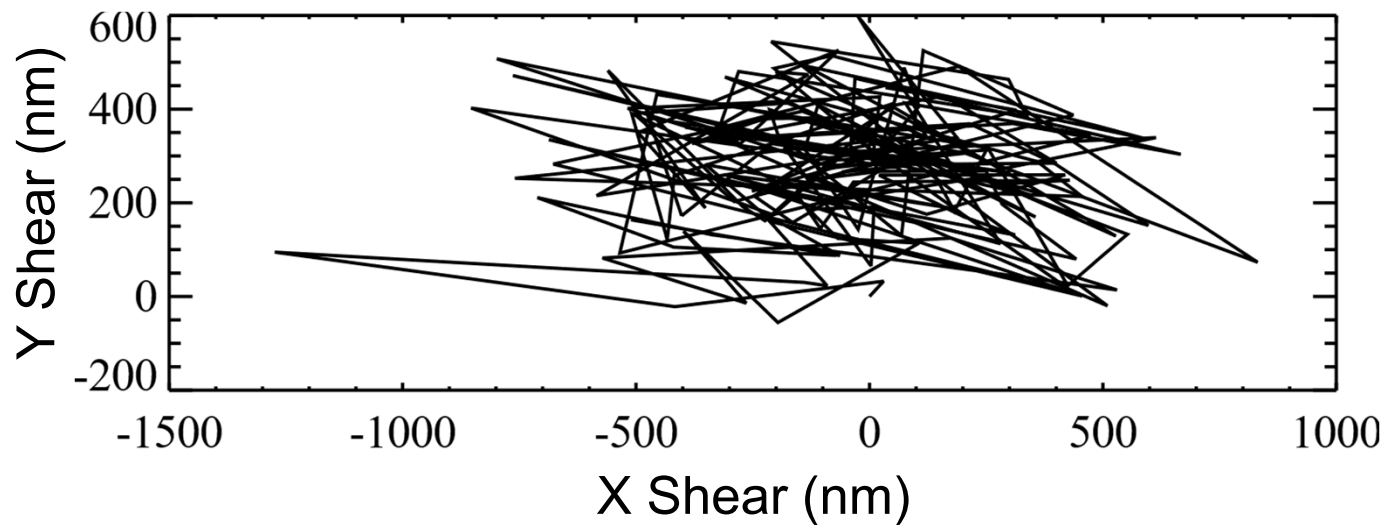
OTA & TCA beam shears
from thermally-induced displacements
(ACS corrected, no jitter)



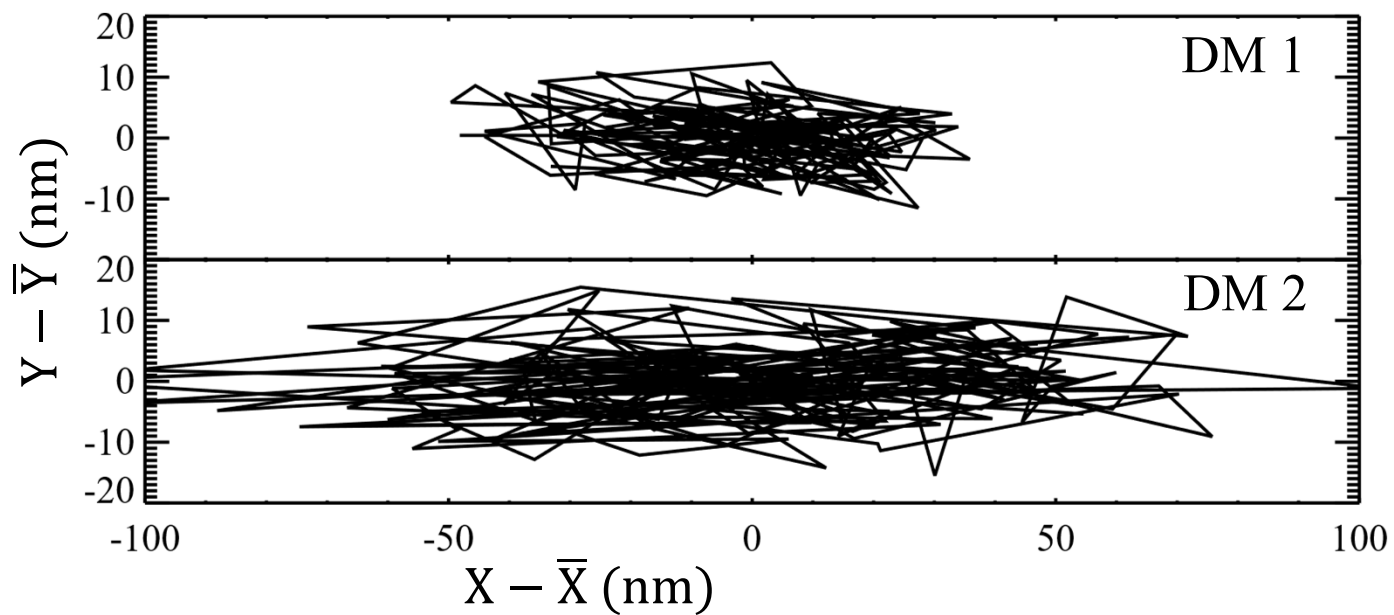
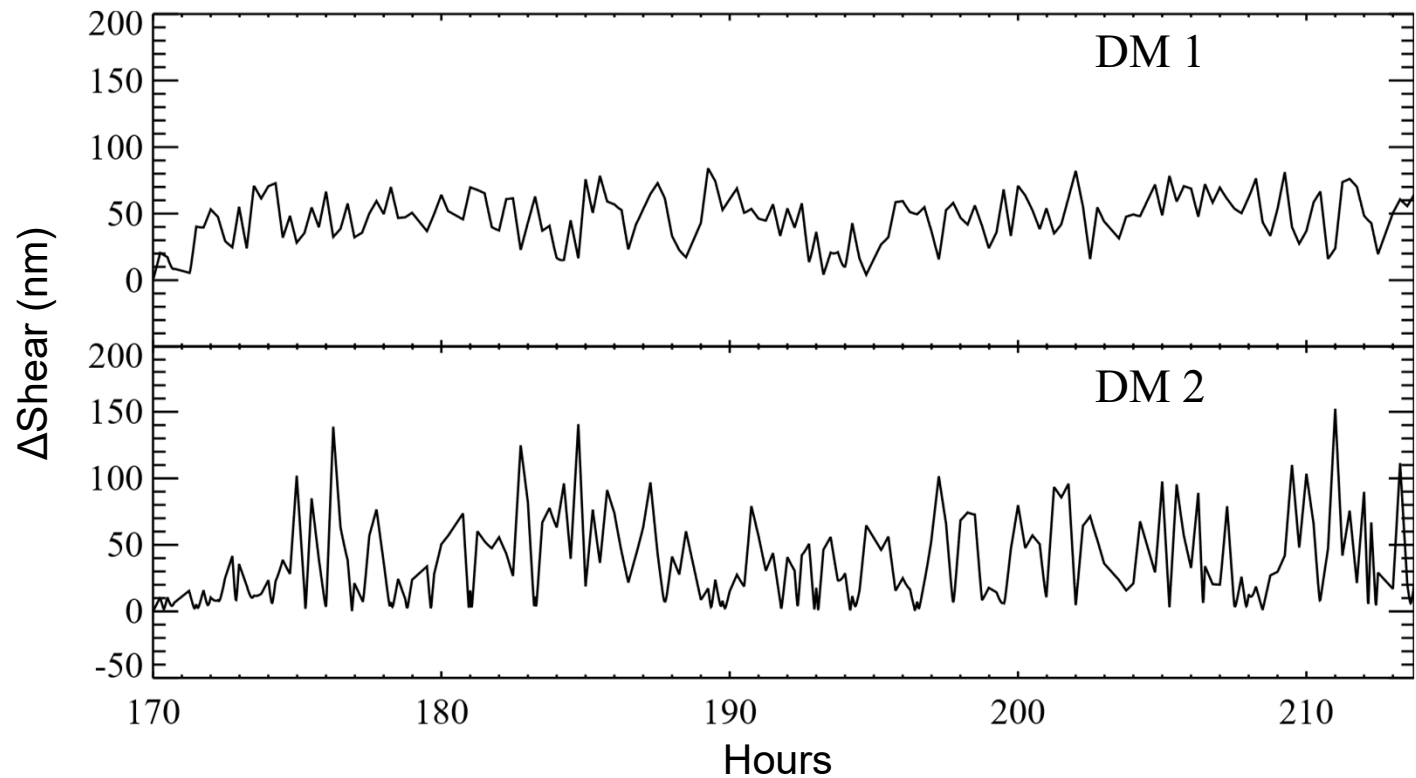
CGI bulk shear (X,Y displacement at FSM relative to instrument carrier)



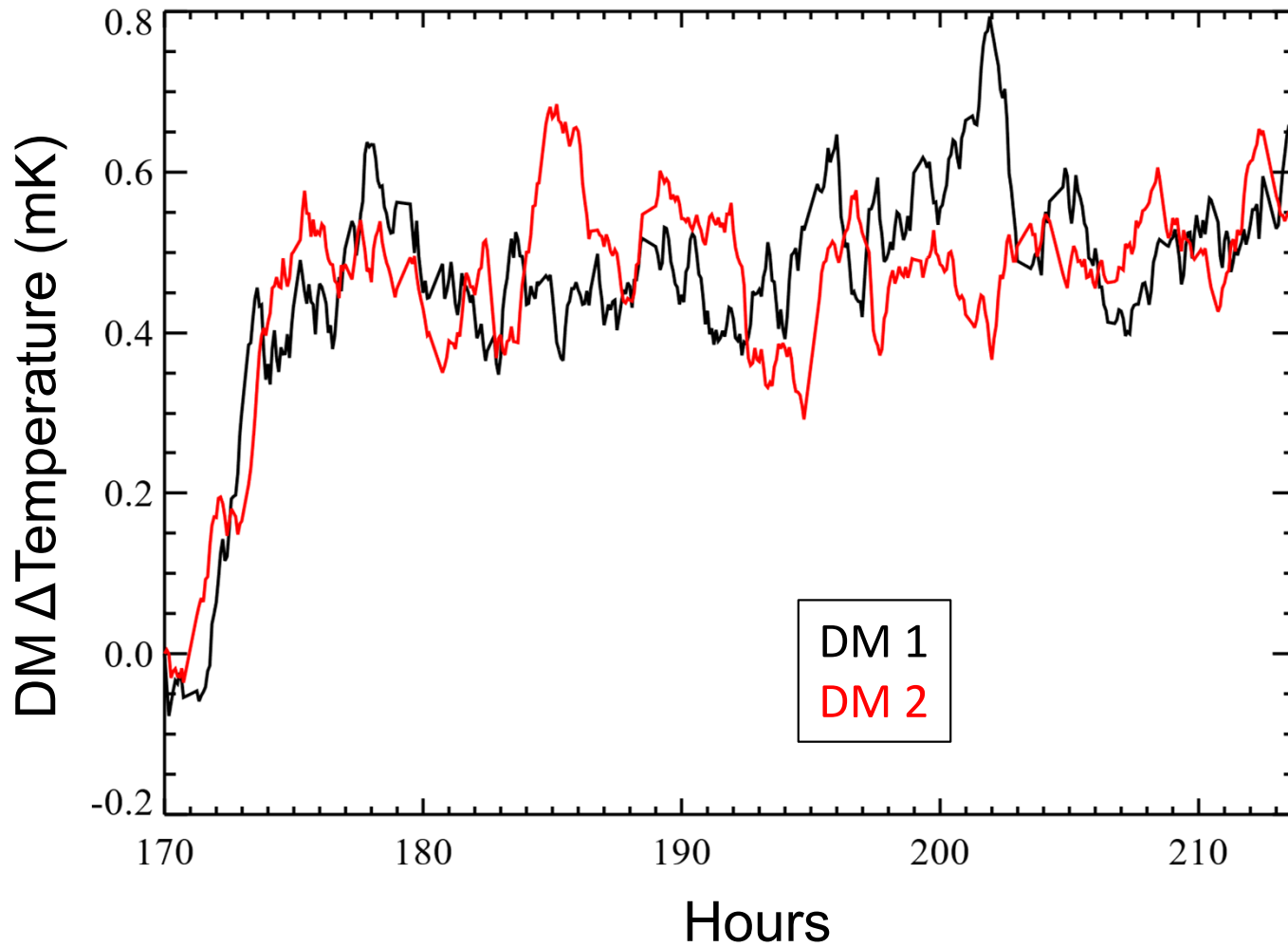
Pupil diameter
@ FSM = 40 mm



DM shear (CGI bulk shear subtracted)



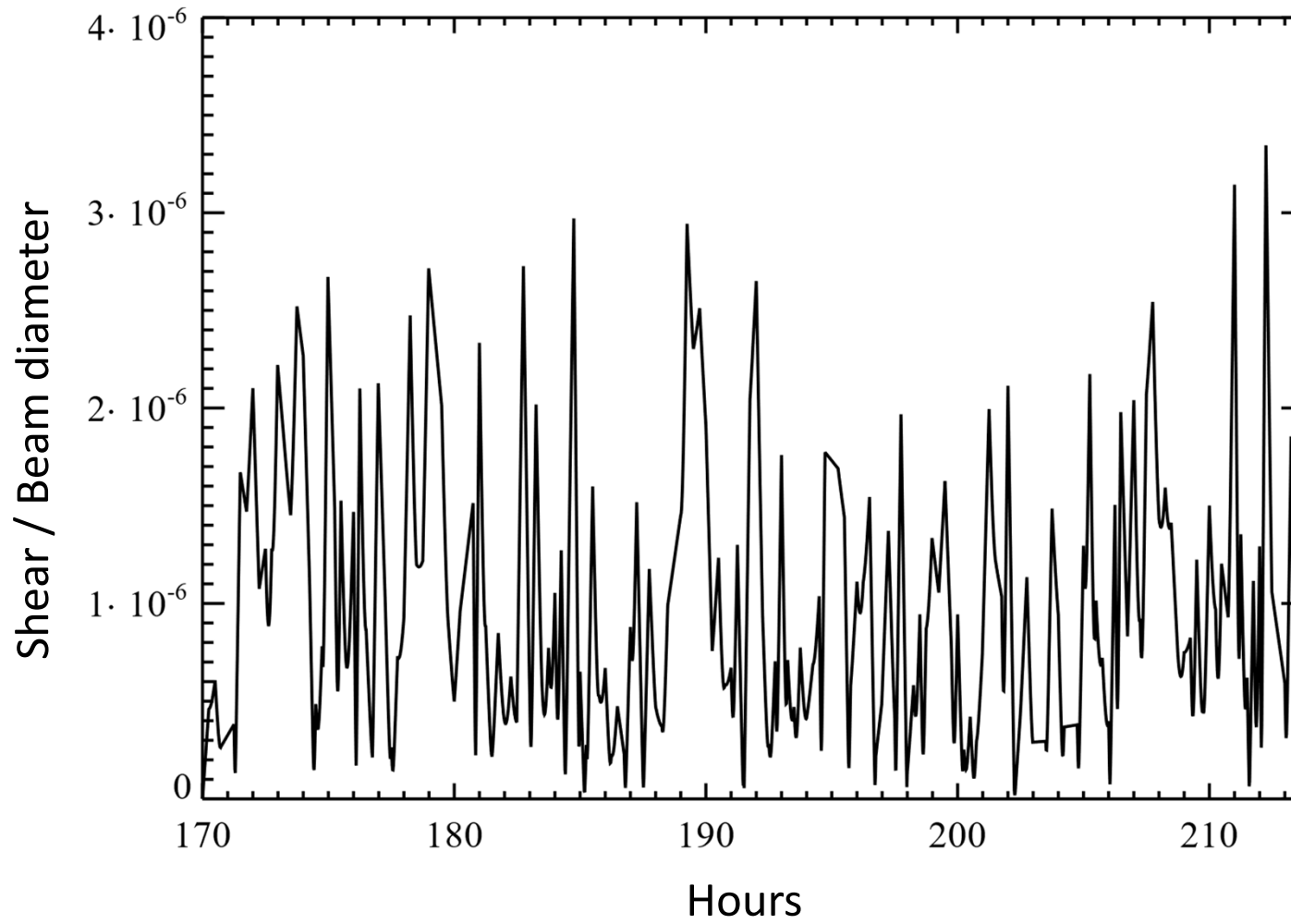
DM temperature change



DM surface change factor = $(1 + 0.026 \times \Delta\text{Temp}_K)$

Max change here is $\sim 0.0021\%$ from $t=170$ h

Lyot stop shear (CGI bulk shear subtracted)



OS11 Reaction Wheel Speeds

